THE EFFECT OF DWELL ON LOW CYCLE FATIGUE IN IMI 829 (Ti 5331S)

J. White, M.H. Loretto and R.E. Smallman, Department of Metallurgy and Materials, University of Birmingham, Birmingham, U.K.
M.R. Winstone, RAE (Pyestock), Farnborough, U.K.

Introduction

Titanium alloys containing significant amounts of α phase have been found to be prone to a marked decrease in low cycle fatigue lifetime associated with the introduction of a period of dwell at maximum load into the fatigue cycle (e.g. (1-3)). This effect is particularly notable in β-processed near-α alloys where the microstructure can consist of large colonies of aligned α platelets within the prior β grains. There is some controversy as to the cause of this effect with various authors advocating the importance of fatigue crack initiation or propagation, texture and the role of impurity elements (particularly hydrogen). It is not, however, the purpose of this paper to review this work but to present the results of a study designed to examine the dislocation structures evolved following fatigue under both dwell and non-dwell conditions.

IMI 829 (also known as Ti 5331S) has been chosen for this specific study for two reasons. Firstly, it is the latest in the current generation of titanium alloys designed for use in high temperature aerospace applications; secondly there is little published work on either the deformation microstructures or the sensitivity to dwell of this alloy.

Initially, the investigation has concentrated on tests conducted at room temperature and these tests form the basis of the present paper. Work at higher temperatures, in the region where strain ageing may be an important factor, is currently underway and it is hoped that the results of this work will be presented in a later paper.

Experimental Procedures

The raw material for this study was supplied by IMI Ltd as 30mm diameter bar taken from a single cast of IMI 829. A cast analysis of the alloying content and the major impurity levels is given in Table 1 along with the nominal composition of the alloy. The bar was heat treated in the β phase field for one hour at 1050°C (1323K) followed by an air cool and a stabilisation treatment for two hours at 625°C (898 K), again followed by an air cool.

	Al	Si	Sn	Zr	Nb	Mo	Fe	Ti
As cast	9.77	0.54	1.42	1.53	0.51	0.13	0.015	bal.
Nominal	9.7	0.5	1.4	1.6	0.5	0.1	-	bal.

Table 1: Cast analysis and nominal composition (at. %).

Test-pieces with a 5mm diameter cross-section were machined from the bar (for full geometry see (4)). The low cycle fatigue tests were performed in tension only, cycling between the maximum load and zero using a triangular waveform at a frequency of ten cycles per minute. Dwell tests incorporated a two minute hold at maximum load into an otherwise identical cycle. Creep tests were also carried out on identical

test-pieces. Three nominal stresses of 800 MPa, 850 MPa and 900 MPa were used, all of the tests being conducted at room temperature. The 0.2% proof stress of this particular batch of IMI 829 was 900 MPa (5).

The broken test-pieces were examined using both optical and scanning electron microscopy (SEM), prior to sectioning to produce thin foils suitable for transmission electron microscopy (TEM). These were prepared by electropolishing discs, 3mm in diameter by 0.4mm thick, cut from the gauge lengths of the test-pieces using spark erosion techniques. The plane of the discs (and therefore the foils) was perpendicular to the tensile axis of the test-piece. Electropolishing was carried out using the method of Blackburn and Williams (6) which has been found to be suitable for most titanium alloys. The thin foils were examined in a Philips EM300, a Philips EM400T (with STEM/EDX attachment) and an EM7 high voltage electron microscope.

Results

The following results are divided into observations made on the heat treated alloy and observations made on the deformed test-pieces.

Observations on the heat treated alloy

The heat treated microstructure of this particular batch of IMI 829 is fully described elsewhere (7) but a brief description of the salient features is pertinent to the observations of the deformed microstructure which are to follow. The optical/SEM microstructure is typical of β-heat treated and air cooled titanium alloys, consisting of colonies of aligned α-platelets within prior β grains (0.4mm in diameter). The TEM microstructure (Figure 1), shows the structure within these colonies. Neighbouring α platelets, which are of similar orientation and ∿2-3μm thick, are separated by thin films of β and/or dislocation networks. Within the platelets themselves the majority of dislocations appear to be randomly orientated with respect to each other and have Burgers vectors of the type $1/3\langle 11\bar{2}0\rangle$ and $1/3\langle 11\bar{2}3\rangle$. In addition, groups of defects exhibiting strong fringe contrast (Figure 2) are occasionally found, usually close to regions of high misorientation (e.g. near colony boundaries). These defects have been shown to be stacking-faults associated with dislocations of Burgers vectors $1/6\langle 20\bar{2}3\rangle$. A full analysis of these faults is presented elsewhere (8) where it has been argued that they are probably growth faults formed during the β to α transformation.

Observations on the deformed test-pieces

(i) General

Graphs of plastic strain against number of cycles/time for the test-pieces deformed using a nominal stress of 800 MPa are shown in Figure 3 (the creep curve has been plotted as if it were a 2 min dwell test). The general trend of these curves is repeated at the higher stresses although the overall magnitude of strain in each case is greater (the total strain for the dwell test-pieces of 850 MPa and 900 MPa were ∿5% and ∿10% respectively).

(ii) Optical/SEM observations

Surface roughening was found to a lesser or greater degree on all test-pieces; this was greatest in the region of final fracture and in

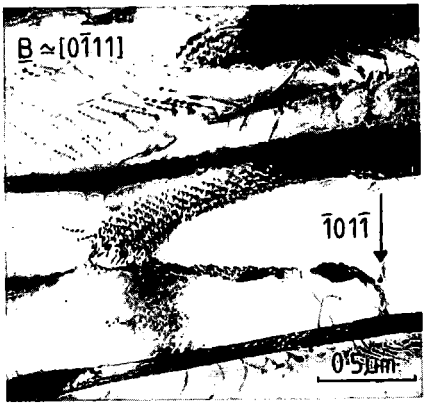

Fig. 1: A bright field TEM micrograph of the undeformed heat treated alloy.

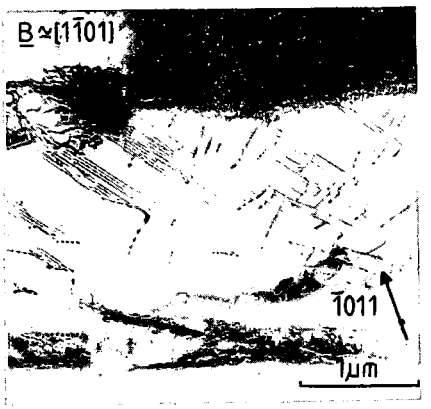

Fig. 2: Fringed defects observed in the undeformed heat treated alloy.

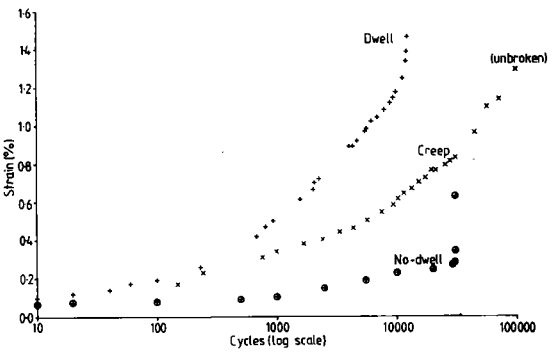

Fig. 3: Plastic strain v. number of cycles/time for dwell, non-dwell and creep at 800 MPa.

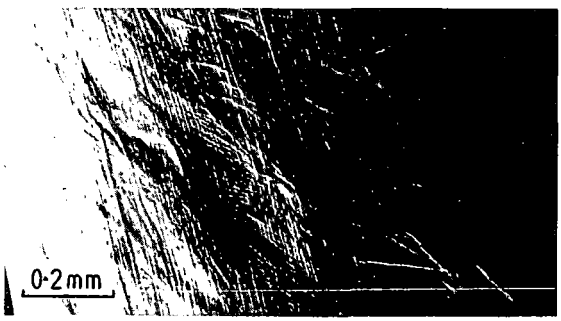

Fig. 4: Deformation on the surface of a test-piece deformed at 850 MPa using a 2min dwell cycle at room temperature.

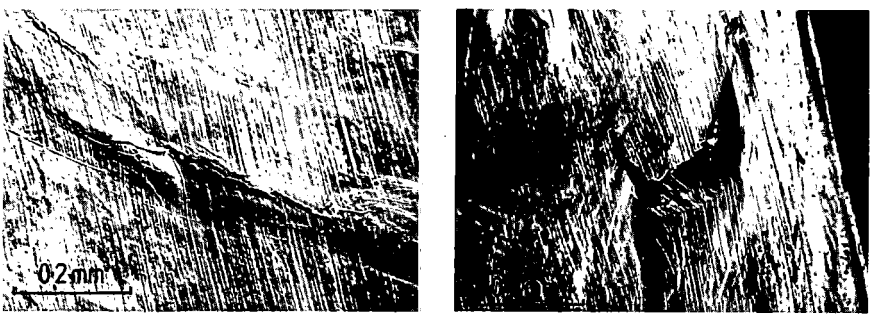

Fig. 5: Surface cracks formed at the surface of a test-piece deformed at 850 MPa using a 2min dwell cycle at room temperature.

Fig. 6: A facetted region on the fracture surface of a test-piece deformed at 900 MPa using a 2min dwell cycle at room temperature (SEM).

those test-pieces which had undergone the highest strains. On closer investigation this roughening was found to be related to the formation of slip traces and the localised deformation of individual grains (Figure 4).

In addition to the surface roughening a number of surface cracks was also observed (e.g. Figure 5). The majority of these were quite straight and often parallel to neighbouring slip traces indicating that they reflected the underlying crystallography. It is particularly notable that they were more prevalent and generally larger in the dwell test-pieces than in the creep and non-dwell test-pieces. An additional experiment, essentially repeating that carried out at 850 MPa with a dwell cycle, showed that (at least for this particular test-piece), the cracks were formed early in the test (at $\sim$25% of the lifetime) with little outward change in their appearance occurring during the remainder of the test.

The fracture surfaces of the broken test-pieces were essentially similar, the overall impression in all cases, being one of a crystallographically related failure. Relatively flat regions (e.g. Figure 6), which had clearly failed with low ductility (often exposing the underlying microstructure) were found on all the fracture surfaces. Although the number and size of these facets altered between test-pieces no systematic variation could be found which correlated with the applied stress or type of deformation employed. Fatigue striations were found in the dwell and non-dwell but not in the creep test-pieces.

(iii) TEM observations

The following observations relate only to the dwell and non-dwell test-pieces, thin foils of the creep test-pieces being unavailable at present. The distribution of deformation was inhomogeneous both within and between foils. Within each foil the variation of dislocation density between α colonies was such that some were completely undeformed. Between foils the average dislocation density was higher in those foils taken from close to the fracture surface. This latter distribution was clearly mirrored in the surface deformation reported earlier which varied in a similar manner.

The deformation-induced dislocations were largely contained within planar slip arrays, these frequently traverse whole α colonies; the intervening β films apparently offering little resistance to their progress. The intersection of slip planes and β often results in displacement of the β along the slip plane (Figure 7).

The most commonly observed $\underline{a}$ type slip systems were $1/3\langle 11\bar{2}0\rangle\{1\bar{1}00\}$ and $1/3\langle 11\bar{2}0\rangle(0001)$, although $\underline{a}$ type dislocations have also been observed which appear to glide on irrational slip planes orientated close to (0001). Generally the slip planes are not singular but exist as groups, for example, Figure 8 shows a group of (0001) slip planes where there are clearly two distinct sets of dislocations (A and B) lying along different directions. These two sets of dislocations have been shown to lie on two distinct (0001) planes and have different Burgers vectors ($\underline{A}=1/3[\bar{2}110]$, $\underline{B}=1/3[1\bar{2}10]$); both sets of dislocations lying close to their respective screw orientations. The other slip plane in Figure 8 is one of the irrational slip planes mentioned earlier and contains dislocations with $\underline{b}=1/3[\bar{2}110]$.

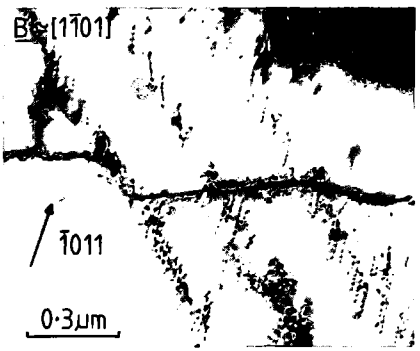

Fig. 7: A bright field TEM micrograph showing the displacement of β by intersecting slip bands in a test-piece deformed at 900 MPa using a 10 cpm fatigue cycle at room temperature.

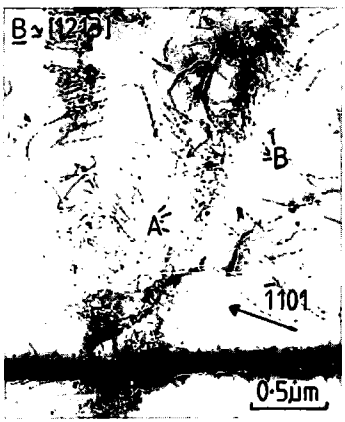

Fig. 8: A bright field TEM micrograph of basal and irrational slip bands in a test-piece deformed at 800 MPa using a 10 cpm fatigue cyle at room temperature.

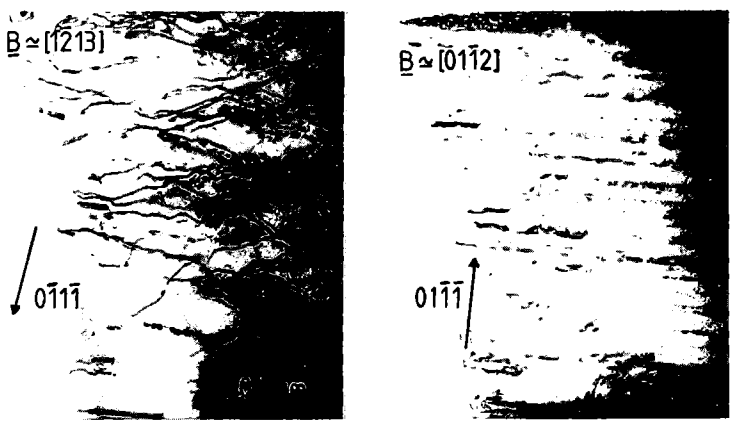

Fig. 9: Bright field TEM micrographs showing 1/3<11$\bar{2}$3> dislocations on (01$\bar{1}\bar{1}$) in a test-piece deformed at 800 MPa using a 10 cpm fatigue cycle at room temperature.

Figure 9 shows an example of a colony deformed by the motion of $1/3\langle 11\bar{2}3\rangle$ dislocations. In this case no a type slip planes could be found in this particular colony however the two types of slip plane are not mutually exclusive. Tilting of the foil showed that the $1/3\langle 11\bar{2}3\rangle$ dislocations were mainly contained within the $\{01\bar{1}1\}$ planes (Fig. 9b); these were not as well defined as with the a type slip planes, there being a number of pinched-off loops and dipoles present indicating that considerable cross-slip had occurred.

A quantitative measurement of the dislocation density was difficult to obtain because of the inhomogeneous distribution of the deformation. However, a relative assessment, arrived at by comparing foils from similar regions of different test-pieces, suggests that the dislocation density increases both with an increase in stress and the introduction of dwell into the fatigue cycle. There is no difference in the character of the slip systems in the dwell and non-dwell test-pieces.

Discussion

The primary objective of the present study has been to compare the deformation microstructures in dwell and non-dwell tested IMI 829. This has been accomplished; the conclusion being that there is no essential difference in the character of the slip systems observed in the two types of test-piece. Although there is a general increase in dislocation density in the dwell compared with the non-dwell test-pieces, this is consistent with the higher level of strain observed in these samples.

Calculations have shown that the difference in strain between the dwell and non-dwell test-pieces observed in this study may not be irreconcilable. If it is assumed that the accumulation of strain in the dwell test-pieces is primarily attributable to the time-dependent deformation accrued during the dwell-on-load part of the fatigue cycle, the resultant empirical relationship between strain, stress and time so derived can be used to calculate the strain expected in the non-dwell test-pieces. Such a calculation gives surprisingly good agreement with the observed strain and suggests that at least in terms of strain accumulation similar processes are operating in both types of test-piece. The observation of essentially identical deformation modes in the TEM supports this conclusion.

A comparison between the creep and dwell strain curves shows, in contrast to the implication of the above calculation, that the rate of strain accumulation in the dwell test-pieces cannot be attributed to creep alone. One possibility is that the higher strain in these test-pieces is related to the observation of surface cracks which, although present in all test-pieces, have been observed to be larger and present in greater numbers in those subjected to dwell. These cracks would increase the effective stress thus giving rise to an increase in strain in the dwell test-pieces relative to that in the creep test-pieces.

Internal cracks in a creep test-piece have been reported by Hack and Leverant (3) in IMI 685. Interestingly their results show dwell and creep tests with similar strain-time curves. This apparent contradiction to the present study may arise as a result of the differences in alloy compositions. It is more likely, however, that it is attributable to differences in experimental technique. Hack and

Leverant used a five minute dwell-time and it is also notable that their overall creep rates were significantly greater than those in the present study. This would suggest that the creep contribution to the deformation of the dwell test-piece was also increased. If this is the case, then by implication, the higher comparitive strain rate seen in the present study must be due to an interaction between creep and fatigue; this may take place through the enhanced nucleation and growth of cracks (both surface and internal) in the dwell test-pieces.

As surface cracks have been found in all three types of test-piece it is a reasonable assumption that there is a natural tendency for this alloy to crack when subjected to stresses of this high order. It is most likely that the crack plane is (0001) in view of the wealth of literature which relates to the susceptibility of titanium alloys to cracking on this plane (mainly concerned with facet formation). There are several possibilities that may account for this phenomenon, perhaps the most likely being the diffusion of an interstitial impurity (e.g. H_2 or O_2) to the basal slip planes. One further possibility can be advanced on the basis of observations made during the present study. It has been observed that basal slip planes can be associated with the basal stacking-faults occasionally found in this alloy. As reported earlier in this paper c component dislocations are associated with these faults. By their very nature these are sessile in the basal plane and thus will present an obstacle to the glide of a type dislocations on that plane. This would result in dislocation pile ups which, it is proposed, may result in the propagation of micro-cracks along the basal plane - the sessile c component dislocation itself being the atomic-sized nucleus of the crack.

Conclusions

(1) There is no significant difference in the deformation modes observed in dwell and non-dwell test-pieces. The comparitively higher average dislocation density observed in the dwell test-pieces is consistent with the higher strain in these compared with the non-dwell test-pieces.

(2) The higher rate of strain-accumulation in the dwell compared with the creep test-pieces may be due to the observation of a greater degree of surface (and possible internal) cracking arising from the interaction of creep and fatigue.

(3) A mechanism that may account for the propensity of titanium and its alloys to crack on the basal plane has been suggested, associated with the presence of c-component stacking-faults on that plane.

Finally the authors would like to acknowledge the Procurement Executive of the Ministry of Defence for financial assistance.

References

(1) D. Eylon, J.A. Hall: Met. Trans. 8A (1977) 982.
(2) W.J. Evans, G.R. Gostelow: Met. Trans. 10A (1979) 1837.
(3) J.E. Hack, G.R. Leverant: Met. Trans. 13A (1982) 1729.
(4) G.S. Harrison, M.J. Weaver: AGARD Conf. Proc. No. 243 (1978).
(5) A.P. Woodfield: Private Communication.
(6) M.J. Blackburn, J.C. Williams: Trans. AIME 239 (1967) 287.
(7) A.P. Woodfield, M.H. Loretto, R.E. Smallman: "Fifth International Conference on Titanium" Munich (1984).
(8) A.P. Woodfield, J. White, M.H. Loretto: to be submitted to Scripta Met.